Biomimetic Synthesis of Lysozyme−Silica Hybrid Hollow Particles Using Sonochemical Treatment: Influence of pH and Lysozyme Concentration on Morphology

Toru Shiomi,[†,‡] Tatsuo Tsunoda,*[,‡] Akiko Kawai,[‡] Fujio Mizukami,[‡] and Kengo Sakaguchi*[,†]

Department of Applied Biological Science, Faculty of Science and Technology, Tokyo University of Science, Noda-shi, Chiba-ken, 278-8510, Japan, and Research Center for Compact Chemical Process, National Institute of Advanced Industrial Science and Technology (AIST), 4-2-1, Nigatake Miyagino-ku, Sendai-shi, Miyagi-ken, 983-8551, Japan

Received April 13, 2007. Revised Manuscript Received June 20, 2007

The silica precipitation activity of lysozyme and the possibility of controlling the resulting particle morphologies were investigated. Lysozyme can act as not only a silica precipitation agent but also as a component of the precipitation products, namely, forming a composite of lysozyme and silica. Stirring produced lysozyme−silica hybrid granular particles (L-SHGs), while a sonochemical treatment resulted in lysozyme−silica hybrid hollow particles (L-SHHs). The silica precipitation activity of lysozyme and the formation of L-SHHs occur only around pH 9. At the optimized pH, the lysozyme concentration was found to affect the morphologies of the L-SHHs. Compared with other basic proteins, the foaming properties of lysozyme appear to be a key factor in the formation of hollow structures. The proposed formation mechanisms of L-SHGs and L-SHHs are also discussed.

Introduction

In recent years, the synthesis of silica has been significantly advanced through a biomimetic approach based on the insights gained into the molecules and mechanisms that enable silica morphogenesis in biological systems such as diatoms and sponges.[1−3] Diatom cell walls and the skeletons of sponges consist of silica. Their intricate silica architectures, which are more complex than those obtained by artificial means, have attracted material scientists to mimic their morphology.[4,5] Two research groups have identified the proteins responsible for the biomineralization formation of silica structures in diatoms and sponges, namely, silaffin and silicatein, respectively.[6,7] Cationic peptides, including derivatives from silaffins (R5 peptide), poly-L-lysine, and polyamines, have also been shown to promote silica condensation in a solution of monosilicic acid.[8−12] Meanwhile, it has been reported that diblock copolypeptides mimicking silicatein can catalyze the hydrolysis of tetraethoxyorthosilicate (TEOS) and its condensation under ambient conditions.[13] The structural complexity and polyfunctionality of the proteins were suggested to be essential to reproduce the shape-controlling ability of silicatein. Such polypeptides and proteins would seem to point to a new materials-science path to the synthesis of differently patterned silica structures. The fact that synthetic peptides and purified proteins from natural biosilica sources cannot be readily obtained will probably restrict their industrial application. Hence, we are exploring alternative proteins for silica biomineralization.

Recently, it has been demonstrated that lysozyme, one of most abundant proteins easily obtained from a commercial source, is effective for biomimetic silica synthesis from alkoxide at ambient temperature and pH.[14] In addition, lysozyme−silica hybrid hollow spheres have been successfully synthesized by the mixing of TEOS with lysozyme in a sonochemical treatment.[15] As well as the economic advantages of this enzyme, the controllable morphologies of such lysozyme−silica composite particles might lead to a biomimetic route for the synthesis of inorganic material. Hollow structures in particular have attracted much attention because of their extensive applications in microencapsulation,

* To whom correspondences should be addressed. E-mail: kengo@rs.noda.tus.ac.jp (K.S.), t.tsunoda@aist.go.jp (T.T.).
† Tokyo University of Science.
‡ AIST.

(1) Sanchez, C.; Arribart, H.; Giraud, G.; Marie, M. *Nat. Mater.* **2005**, *4*, 277−288.
(2) M*v*ller, W. E. G. *Silicon Biomineralization*; 2003; Vol. 33.
(3) Sun, Q.; Vrieling, E. G.; van Santen, R. A.; Sommerdijk, N. A. J. M. *Curr. Opin. Solid State Mater. Sci.* **2004**, *8*, 111−120.
(4) Foo, C. W. P.; Huang, J.; Kaplan, D. L. *Trends Biotechnol.* **2004**, *22*, 577−585.
(5) Sumper, M.; Brunner, E. *Adv. Funct. Mater.* **2006**, *16*, 17−26.
(6) Shimizu, K.; Cha, J.; Stucky, G. D.; Morse, D. E. *PNAS* **1998**, *95*, 6234−6238.
(7) Kroger, N.; Deutzmann, R.; Sumper, M. *Science* **1999**, *286*, 1129−1132.
(8) Knecht, M. R.; Wright, D. W. *Chem. Commun.* **2003**, 3038−3039.
(9) Sumper, M. *Angew. Chem., Int. Ed.* **2004**, *43*, 2251−2254.
(10) Rodriguez, F.; Glawe, D. D.; Naik, R. R.; Hallinan, K. P.; Stone, M. O. *Biomacromolecules* **2004**, *5*, 261−265.
(11) Mizutani, T.; Nagase, H.; Fujiwara, N.; Ogoshi, H *Bull. Chem. Soc. Jpn.* **1998**, *71*, 2017−2022.
(12) Tomczak, M. M.; Glawe, D. D.; Drummy, L. F.; Lawrence, C. G.; Stone, M. O.; Perry, C. C.; Pochan, D. J.; Deming, T. J.; Naik, R. R. *J. Am. Chem. Soc.* **2005**, *127*, 12577−12582.
(13) Cha, J. N.; Stucky, G. D.; Morse, D. E.; Deming, T. J. *Nature* **2000**, *403*, 289−292.
(14) Luckarift, H. R.; Dickerson, M. B.; Sandhage, K. H. *Small* **2006**, *2*, 640−643.
(15) Shiomi, T.; Tsunoda, T.; Kawai, A.; Chiku, H.; Mizukami, F.; Sakaguchi, K. *Chem. Commun.* **2005**, 5325−5327.

10.1021/cm071011v CCC: $37.00
Published on Web 08/01/2007

drug delivery systems, and chromatographic carriers.[16−18] Sonochemical syntheses of inorganic hollow particles have been reported by many researchers.[19−21] However, to the best of our knowledge, the combination of biomimetic synthesis and sonochemical treatment has not yet been explored. A number of papers have described various synthesis routes to produce hollow particles of silica, organic polymers, and their composites, which are based on sacrificial template core techniques,[22] layer-by-layer techniques,[23] and W/O emulsion methods using surfactants for stabilizing the organic phase.[24] Unlike these previous approaches, our combination approach described here requires neither removal of the template materials nor repetition of the coating processes. We should also note that it is commonly seen that biosilica in nature occlude biopolymers such as proteins; such interactions many play an important role in the formation of an organic−inorganic composite matrix.[25−27] Lysozyme may play a similar role as that of such biomineralization-related biopolymers during the formation of lysozyme−silica hybrid particles, which may lead to environmentally friendly synthetic processes for structured materials with controlled intricate morphologies.

The important feature of this work is the compatibility of silica biomineralization and morphological control of lysozyme−silica hybrid particles using a sonochemical treatment. The precipitation of silica from TEOS is promoted by lysozyme under ambient buffer conditions. Lysozyme can also serve as parts of resultant hollow particles and granular ones. We here not only report the influence of reaction conditions on the morphologies of lysozyme−silica hybrid particles but also discuss the formation mechanism of hollow structures. The manner of mechanical agitation, the pH, and the initial lysozyme concentration in the synthesis solution are all key factors in the formation of lysozyme−silica hybrid hollow particles (L-SHHs).

Experimental Section

Chemicals. All chemicals used in this paper were commercially available and were used without further purification. Lyophilized lysozyme from chicken egg whites for biochemistry grade and other chemical compounds and proteins [cytochrome C, hemoglobin, β-amylase, and bovine serum albumin (BSA)] were purchased from Wako Pure Chemical Industry, Ltd. Ribonuclease A and apo-transferrin were purchased from Sigma.

(16) Radt, B.; Smith, T. A.; Caruso, F. *Adv. Mater.* **2004**, *16*, 2184−2189.
(17) Caruso, F. *Chem.—Eur. J.* **2000**, *6*, 413−419.
(18) Sakai, S.; Ono, T.; Ijima, H.; Kawakami, K. *Biomaterials* **2001**, *22*, 2827−2834.
(19) Wang, S. F.; Gu, F.; Lu, M. K. *Langmuir* **2006**, *22*, 398−401.
(20) Zhu, J. J.; Xu, S.; Wang, H.; Zhu, J. M.; Chen, H.-Y. *Adv. Mater.* **2003**, *15*, 156−159.
(21) Dhas, N. A.; Suslick, K. S. *J. Am. Chem. Soc.* **2005**, *127*, 2368−2369.
(22) Sun, X.; Liu, J.; Li, Y. *Chem.—Eur. J.* **2006**, *12*, 2039−2047.
(23) Caruso, F.; Caruso, R. A.; Mohwald, H. *Science* **1998**, *282*, 1111−1114.
(24) Fujiwara, M.; Shiokawa, K.; Tanaka, Y.; Nakahara, Y. *Chem. Mater.* **2004**, *16*, 5420−5426.
(25) Hecky, R. E.; Mopper, K.; Kilham, P.; Degens, E. T. *Mar. Biol. (Heidelberg, Ger.)* **1973**, *19*, 323−331.
(26) Perry, C. C.; Keeling-Tucker, T. *J. Biol. Inorg. Chem.* **2000**, *5*, 537−550.
(27) Noll, F.; Sumper, M.; Hampp, N. *Nano Lett.* **2002**, *2*, 91−95.

Table 1. Silica Precipitating Ability of Various Proteins

protein	pI	silica precipitation/mg
lysozyme	11	5.46 ± 0.05
cytochrome C	10.1	7.34 ± 0.13
ribonuclease A	9.5	5.62 ± 0.05
hemoglobin	7	<0.01
β-amylase	6.5	<0.01
apo-transferrin	5.9	no precipitation observed
BSA	5.5	no precipitation observed
no protein		no precipitation observed

Preparation of Lysozyme−Silica Hybrid Hollow Particles (L-SHHs) and Lysozyme−Silica Hybrid Granular Particles (L-SHGs). In a typical synthesis, a lysozyme solution of the desired concentration was prepared by dissolving lyophilized lysozyme powder into a 0.05 M glycine buffer, after which the pH was adjusted to 9.0 by 5 N NaOH. A total of 1 mL of TEOS was added to 9 mL of the lysozyme solution, and immediately the mixture was sonicated on a bath type sonicator operated at a constant-output frequency of 42 kHz and an output power of 90 W (Branson1510, Yamato) or stirred for 15 min at room temperature (RT). The resultant solutions were dispensed onto a polystyrene plate and dried at 60 °C for 24 h, after which a white powder was obtained. As well as lysozyme, the synthesis was also carried out with cytochrome C and ribonuclease A. A stirring device outfitted with a propeller and a probe-type sonicator (Branson Sonifier 250) were also used to agitate the reaction mixture in place of a bath-type sonicator. The microtip of a probe-type sonicator was positioned in 40 mL of the reaction mixture in a 50 mL polypropylene tube, and subsequently ultrasound irradiation was applied at a constant-output frequency of 20 kHz and minimum output power of 10 W. Stirring with a propeller was performed at a rotation frequency of 1000 rpm.

Characterization of L-SHHs and L-SHGs. Scanning electron microscope (SEM) images of L-SHHs were measured using a JEOL JSM-5310LV at 15 kV and 33 Pa in a low-vacuum mode without metal coating. High-resolution SEM images were measured using a Hitachi S-800 operated at 10 kV with a platinum coating. The elemental analysis was recorded with an energy dispersive X-ray (EDX) analyzer (KEVEX Delta series) mounted on the Hitachi S-800. Transmission electron microscopy (TEM) was performed on a JEM-2010F microscope (JEOL) operating at 200 kV. The nitrogen adsorption/desorption experiments were carried out using a NOVA 3000 series (Quantachrome Instruments) instrument, before which L-SHHs and L-SHGs were dried at 60 °C for 24 h. Infrared radiation (IR) spectra of pellet samples diluted with KBr were recorded on a FT-IR 410 (JASCO; FT-IR = Fourier-transform infrared). The thermal gravimetric analysis (TGA) was recorded on a TG/DTA 300 instrument (SEIKO) at 10 °C min^{-1} in an air atmosphere.

Quantitative Determination of Synthesized L-SHHs. The silica precipitation activity of lysozyme was determined by weighing the amount of precipitates. L-SHHs were precipitated by centrifuging at 12 000 rpm for 15 min after the sonicated mixture was left under static conditions at RT for an appropriate time. The precipitate was washed with 50% ethanol twice and dried at 60 °C. The weight of the obtained dry sample powder per 1 mL of reaction solution was measured in triplicate. The same L-SHH precipitation samples were used for further analysis by SEM, FT-IR, and TGA. The silica precipitation activity of other proteins was also determined in the same way.

Results and Discussion

Silica Precipitation Activity of Various Proteins. Table 1 shows the silica precipitation activity from TEOS for

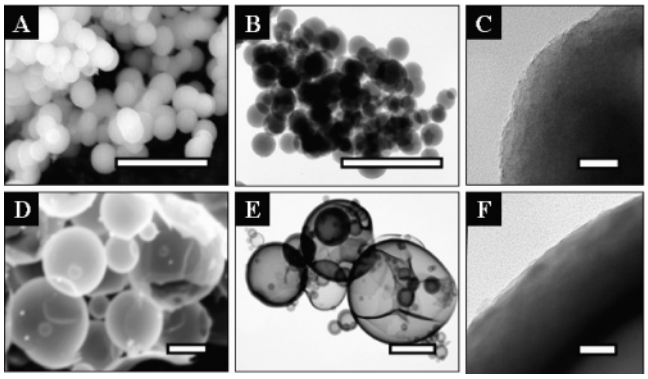

Figure 1. SEM and TEM images of L-SHGs (A−C) and L-SHHs (D−F). Scale bars: (A, B, D, E) 3 μm, (C and F) 50 nm.

various proteins (each protein concentration: 5 mg mL^{-1}). Proteins with basic pI have silica precipitation activity. On the other hand, almost no precipitation was observed for hemoglobin and proteins with acidic pI. A control experiment, carried out using the same reaction solution without any protein, resulted in no precipitation. These results suggest that the total positive net charge and cationic residues of the basic proteins that accelerate silica precipitation play important roles under the conditions employed (pH 9.0, 0.05 M glycine buffer). As lysozyme is cheap and easy to obtain, the effect of the reaction conditions such as agitation, substrate and protein concentration, and so forth on the silica precipitation rate and morphologies of the precipitates was investigated in detail with this protein.

Synthesis of L-SHHs (Lysozyme−Silica Hybrid Hollow Particles) and L-SHGs (Lysozyme−Silica Hybrid Granular Particles). Lysozyme is a small basic protein (MW ≈ 14 000, pI ≈ 11.0) with an amino acid sequence of predominantly basic residues (lysine, arginine, and histidine) and hydroxyl residues (serine and tyrosine)[28] which may be responsible for the interaction between silica or silica precursors and polypeptides.[29,30] To examine the effect of the agitation method on the morphologies of the precipitates, TEOS was mixed with a lysozyme solution (0.05 M glycine buffer, pH 9.0, final lysozyme concentration of 2.0 mg mL^{-1}) for 15 min at RT under stirring (L-SHGs) or sonication (L-SHHs). The resultant mixture was dried up at 60 °C for 24 h to yield white precipitation products.

The SEM image in Figure 1A shows that L-SHGs have a spherical shape with an average particle diameter of 660 nm. Figure 1B and C are the TEM images of L-SHGs. They formed densely packed spherical particles without any specific contrast derived from the aggregation of lysozyme or silica particles. When sonication was used to agitate the solution instead of mechanical stirring, the morphology of the products changed. As shown in Figure 1D and E, L-SHHs exhibited a hollow spherical structure with a diameter of 0.5−15 μm, and the shell wall thickness was approximately 100 nm, or more. For both types of particles, higher-magnification images of their walls did not show any characteristic contrast of cluster structure (Figure 1F). From

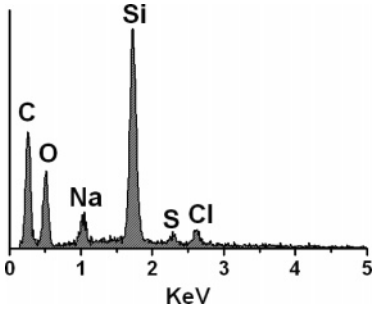

Figure 2. Typical results of EDX analysis of L-SHHs.

the selected-area electron diffraction patterns, both L-SHGs and L-SHHs were indicated to be amorphous, as has been previously reported for natural biogenic silica and biomimetic silica.[31,32]

Figure 2 is a representative result of the EDX analysis of L-SHHs. The presence of the silica structure was clearly confirmed from the Si main signal. The sulfur signal is diagnostic for lysozyme, indicating that L-SHHs are composed of lysozyme and silica. In other words, lysozyme is more than a simple silica precipitation agent; it becomes a component part of L-SHHs. The Na and Cl signals derived from buffer constituents of the reaction solution were also detected. These elements might exist within the lysozyme−silica hybrid network playing roles as connectors between silica and the lysozyme molecule, or they may merely be present on the L-SHH's surface. Considering the homogeneous structure of L-SHHs observed by TEM (Figure 1F), lysozyme seems to be uniformly distributed within the silica matrix.

An EDX analysis of L-SHGs exhibited similar elemental composition peaks and provided evidence that this hybrid matrix model is also valid for L-SHGs. These results suggest that the different mechanical agitations affect only the morphology of the product, keeping the composition of lysozyme and silica unchanged. Thus, other methods of mechanical agitations were tried using a stirring device outfitted with a propeller and a probe-type sonicator. Although precipitate was obtained in all attempts, hollow structures were not formed through these synthesis routes. SEM observations revealed that only fragmented shell structures or aggregations of fragments were formed. These failures appeared to be caused by the mechanical collapse of intermediate products. Because TEOS is not miscible with water, all agitation methods can easily generate TEOS emulsions dispersed within the water phase. However, when a stirring device is used, the growing hollow structure is collapsed by the shear stress induced by the propeller. Sonochemical irradiation by a probe-type sonicator can directly transfer the output power to the reaction mixture without attenuation, which is therefore probably much more efficient than a bath-type sonicator, leading to the collapse and aggregation of growing hollow structures. Therefore, the emulsions did not grow into hollow structures for any type of mechanical agitation other than sonication using a bath-

(28) Canfield, R. E.; Liu, A. K. *J. Biol. Chem.* **1965**, *240*, 1997−2002.
(29) Zhou, Y.; Shimizu, K.; Cha, J. N.; Stucky, G. D.; Morse, D. E. *Angew. Chem., Int. Ed.* **1999**, *38*, 779−782.
(30) Coradin, T.; Livage, J. *Colloids Surf., B* **2001**, *21*, 329−336.
(31) Vrieling, E. G.; Beelen, T. P. M.; van Santen, R. A.; Gieskes, W. W. C. *J. Phycol.* **2000**, *36*, 146−159.
(32) Sun, Q.; Beelen, T. P. M.; van Santen, R. A.; Hazelaar, S.; Vrieling, E. G.; Gieskes, W. W. C. *J. Phys. Chem. B* **2002**, *106*, 11539−11548.

type sonicator. From these results, it is apparent that the use of sonochemical irradiation at an appropriately controlled power level is essential for the formation of hollow spherical particles. The precise control of the sonochemical power may contribute to the morphological control of hollow structure.

Influence of pH on the Formation of Hollow Structures. Another key point to investigate concerning the formation of hollow structures is whether, and how, lysozyme molecules interact with TEOS emulsion and silica species. In this regard, we focused in the following experiments on changes in the reaction solution conditions. One of the parameters controlling the interaction between lysozyme and silica (TEOS) is the pH value. It has been known that the net charge of both silicate species and lysozyme molecules changes in different pH solutions.[33] Hence, to obtain a clue to help solve the formation mechanism of L-SHHs, the precipitation behavior using a series of lysozyme solutions at different pHs were examined. In Figure 3A, it can be readily seen with the naked eye that the mixed TEOS/lysozyme solutions of pH 5.0−9.0 were turbid within 3 min after a sonochemical treatment. Only slight turbidity was observed for solutions with pH 11.0 and 12.6. When the solutions were allowed to stand for 12 h, white precipitates were observed above pH 7.7. In contrast, on standing, the turbid solutions of pH 5.0 and 6.7 turned clear and did not produce any precipitates.

The yield of precipitate was determined as a function of reaction time for each pH value of the initial lysozyme solution (Figure 3B). Above pH 11.0, the amount of precipitate linearly increases with increasing reaction time. However, interestingly, a plateau in the amount of precipitates appeared at an early stage for pH 7.7 and 9.0, suggesting that the encapsulation of lysozyme molecules into the silica matrix proceeded as soon as the silica precipitation was instigated by the lysozyme. Such encapsulated lysozyme molecules are restricted from further contact with other TEOS molecules and silica.[34] Thus, the action of lysozyme for the coagulation of silica ends when all the lysozyme molecules become surrounded by silica. Parts C−E of Figure 3 are the SEM images of precipitates obtained in this set of experiments. Although slightly deformed hollow particles could be seen at pH 9.0 (Figure 3C), probably from washing with ethanol, only aggregated forms of primary silica particles were observed at pH 11.0 and 12.6 (Figure 3D and E).

These results from experiments varying the pH can be divided to three groups (at pH < 7, 7 < pH < 11, and 11 < pH). The difference among the groups can be explained by the net charges of lysozyme and silicate species, which are associated with the hydrophobic and electrostatic interactions. Below pH 7, the primary particles of silica are formed very slowly, even if the silicate species could be generated in the absence of lysozyme.[35] Silicate species bear a very weak charge,[33] and lysozyme molecules are positively charged. Hence, the electrostatic interaction between lysozyme and

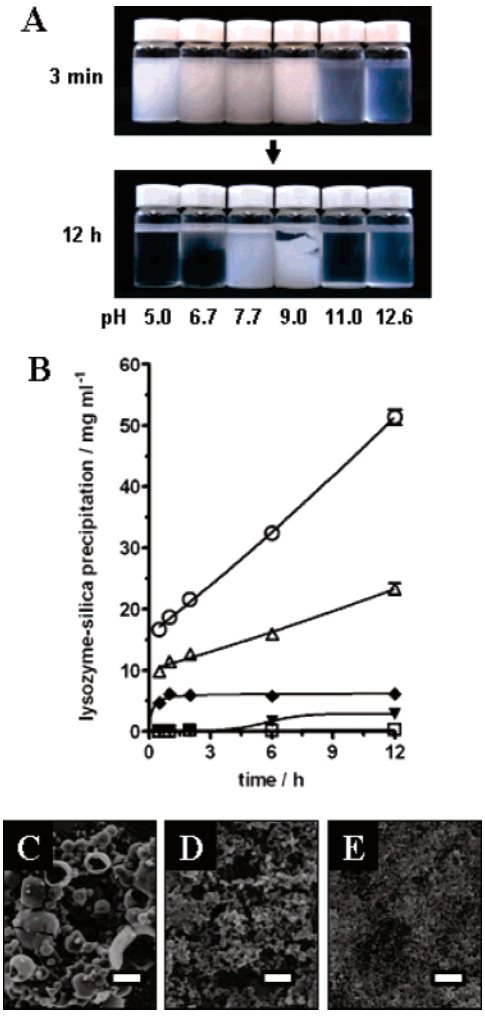

Figure 3. (A) Visible changes of ultrasonically dispersed TEOS/silicate species in the lysozyme solutions at various pH values. (B) Polycondensation and precipitation of lysozyme/silica hybrid as a function of time in the lysozyme solution with pH: (□) 6.7, (▼) 7.7, (◆) 9.0, (△) 11.0, (○) 12.6. (C−E) SEM images of precipitates (pH = 9.0, 11.0, 12.6, respectively) which were allowed to stand for 2 h after the sonication treatment. Scale bars: (C) 10 μm, (D and E) 1 μm. The precipitates were obtained by centrifuging 1 mL of the sample mixture and were washed repeatedly with 50% ethanol.

silica species would be very weak. Hydrophobic interactions between the lysozyme and the TEOS emlusion are also weakened in the low-pH solution, which is far from the pI of lysozyme. Therefore, silica condensation would be little mediated by lysozyme.

At pH 7−11, silica species are negatively charged, so that they interact favorably with positively charged lysozyme.[33] On the other hand, the degree of hydrophobicity of lysozyme seems to increase with increasing pH, at values below its pI. Thus, lysozyme can interact with silicate species and TEOS during the growth of silica structures through electrostatic and hydrophobic interactions. These multiple interactions between lysozyme and silica (TEOS) probably play a key role in the coagulation of silica with lysozyme or the formation of L-SHHs (Figure 3C). In contrast, above pH 11, lysozyme has a negative net charge, causing a repulsive force between silica species and lysozyme.[36] Additionally, the pH

(33) Coradin, T.; Coupe, A.; Livage, J. *Colloids Surf., B* **2003**, *29*, 189−196.
(34) Gill, I.; Ballesteros, A. *Trends Biotechnol.* **2000**, *18*, 282−296.
(35) Iler, R. K. *The Chemistry of Silica*; Wiley: New York, 1979.
(36) Vinu, A.; Murugesan, V.; Hartmann, M. *J. Phys. Chem. B* **2004**, *108*, 7323−7330.

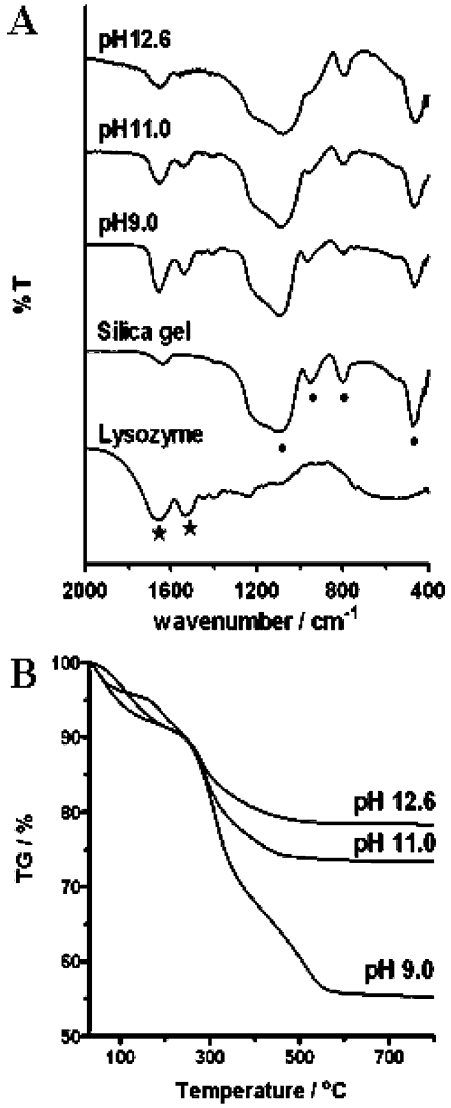

Figure 4. (A) FT-IR spectrum of silica gel, lysozyme powder, and washed precipitates obtained at three pH values. Filled circle (●) and filled star (★) show silica and protein vibrational bands, respectively. (B) TGA analysis of washed precipitates obtained at the same pH's.

value is high enough to allow TEOS to be hydrolyzed by a basic catalyst, followed by silica polymerization and subsequent growth of three-dimensional gel networks (Figure 3D and E). The linear increase in the amount of the precipitate above pH 11 reflects this sol−gel process unassisted by lysozyme (Figure 3B).

To examine whether lysozyme molecules are responsible for the coaggregation at the pH leading to the formation of precipitates, the solids obtained were characterized by FT-IR and TGA. In Figure 4A, the IR spectra of all precipitates showed the characteristic bands of silica at 460 (Si−O−Si bend), 780 (Si−O−Si symmetric stretch), 970 (Si−OH stretch), and 1080 and 1200 cm^{-1} (Si−O−Si antisymmetric stretches).[37] The amide I (C═O/C−N stretch) peak at 1650 cm^{-1} and amide II (N−H bend/C−H stretch) peak at 1540 cm^{-1} corresponding to vibrations of the polypeptide chain of lysozyme can be observed for the precipitate obtained at pH 9.0. The position and relative intensity of the amide I and II bands reflect conformational changes in the protein secondary structure.[38] This spectral characteristic indicates that the secondary structure of lysozyme is maintained within L-SHHs. However, as pH increases, the intensity of amide I and II bands corresponding to the vibrations of the polypeptide chain of lysozyme decreases compared to the intensity of the band at 1080 cm^{-1}, meaning that the percentages of lysozyme within the precipitates at pH 11 and 12.6 are less than that at pH 9.0.

Additional evidence comes from TGA profiles, which showed weight losses due to the lysozyme encapsulated within the precipitates obtained (Figure 4B). Total weight losses for the precipitates obtained at pH 9.0, 11.0, and 12.6 between 200 and 550 °C were 36, 17, and 12%, respectively. The weight losses agree with the above results of FT-IR, although the weight losses in this temperature range possibly include those due to hydrated water and buffer constituents (glycine) as well as lysozyme molecules. Furthermore, it should be noted that, depending on the precipitates, the end point of weight loss shifts to 450 °C (pH 11.0 and 12.6) from 550 °C (pH 9.0). These results indicate that the lysozyme encapsulated into the precipitates at pH 9.0 is more stable against pyrolysis than that remaining on the silica precipitates obtained at pH 11.0 and 12.6. The stable environment is probably provided by the intimate relation between lysozyme and the silica matrix of precipitates obtained at pH 9.0, a result which was also deduced from the relatively high amount of precipitates. Thus, it is reasonable to assume that only at about pH 9 does lysozyme serve as a coaggregation factor and is it tightly encapsulated within the silica matrix.

Influence of Lysozyme Concentration on the Amount and the Morphology of Precipitates. On the basis of the fact that lysozyme molecules are encapsulated within L-SHHs, it is of particular interest to investigate how the lysozyme concentration affects the yield and the morphology of precipitates. The yield of the lysozyme−silica hybrid and the amount of lysozyme remaining in the supernatant were determined as a function of reaction time after sonochemical treatment for the solutions with different initial lysozyme concentrations at pH 9.0 (Figure 5). In the absence of lysozyme, precipitation did not occur at all even after 24 h (Figure 5A). Below a lysozyme concentration of 5.0 mg mL^{-}, the amount of precipitates increases almost proportionally with the concentration of lysozyme applied. The consumption of lysozyme in the reaction mixture is synchronized with the increase of the precipitation amount (Figure 5B). However, the formation rate of precipitates becomes slow with an increase in lysozyme concentration for the solutions with initial concentrations above 5 mg mL^{-1} and reaches the maximal value with the 20 mg mL^{-1} solution (Figure 5A), even though lysozyme remained in the reaction mixture (Figure 5B). This suggests that the surface of the TEOS emulsion was entirely covered with lysozyme molecules in the solutions above 20 mg mL^{-1}. Therefore, the contact area of TEOS with lysozyme molecules acts as a limiting factor for the formation amount of precipitates. The

(37) Ma, D.; Li, M.; Patil, A. J.; Mann, S. *Adv. Mater.* **2004**, *16*, 1838−1841.

(38) Ding, H.-M.; Shao, L.; Liu, R.-J.; Xiao, Q.-G.; Chen, J.-F. *J. Colloid Interface Sci.* **2005**, *290*, 102−106.

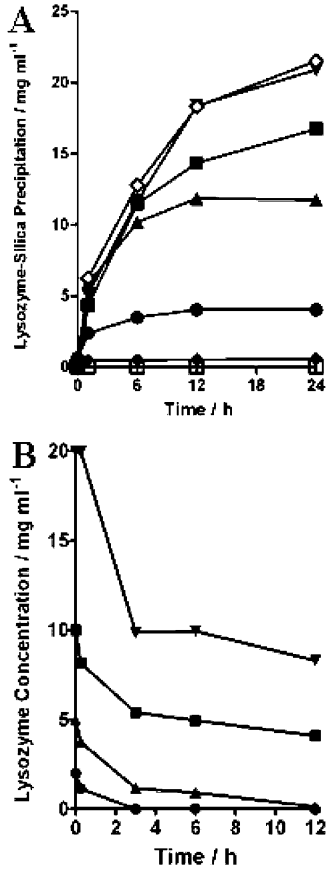

Figure 5. (A) The formation rate of L-SHHs precipitates obtained at different lysozyme concentrations: no lysozyme (□) and 0.5 (◆), 2 (●), 5 (▲), 10 (■), 20 (▼), and 40 mg mL^{-1}(◇). (B) Lysozyme concentration in the supernatants of reaction mixtures after removing L-SHHs precipitates. Lysozyme concentration was determined by a Bradford protein assay.

lysozyme concentration effects were also reflected in the L-SHH morphologies. As showed in Figure 6, an increase in average particle size of L-SHHs was observed below 5 mg mL^{-1} (Figure 6A−C). The observed maximal diameter of L-SHHs retaining its innate hollow structure was about 20 μm. Although the particle size distribution seemed not to change above 5 mg mL^{-1} (Figure C and D), some aggregation forms started to appear among L-SHHs at a concentration of lysozyme of 20 mg mL^{-1} (Figure 6E). The spongelike structure was partially observed at a lysozyme concentration of 40 mg mL^{-1} (Figure 6F).

For comparison, the effect of two basic proteins, cytochrome C and ribonuclease A, on the morphologies of their precipitates was also investigated at different protein concentrations. Unexpectedly, when the initial concentration of each protein solution was 2 mg mL^{-1}, SEM showed the presence of spongelike structures instead of hollow spherical particles (Figure 7A and B). However, when the concentration was 10 mg mL^{-1}, hollow particles formed, but only for ribonuclease A, plus some granular particles indicated by arrows in the SEM image (Figure 7C). The observed correlation between the concentration and morphology of these proteins is in contradiction to that of lysozyme. It is known that lysozyme displays a relatively large hydrophobic patch on its surface which contributes to its foaming property, whereas the hydrophobic residues of ribonuclease A are more or less evenly distributed over the surface.[39] At low

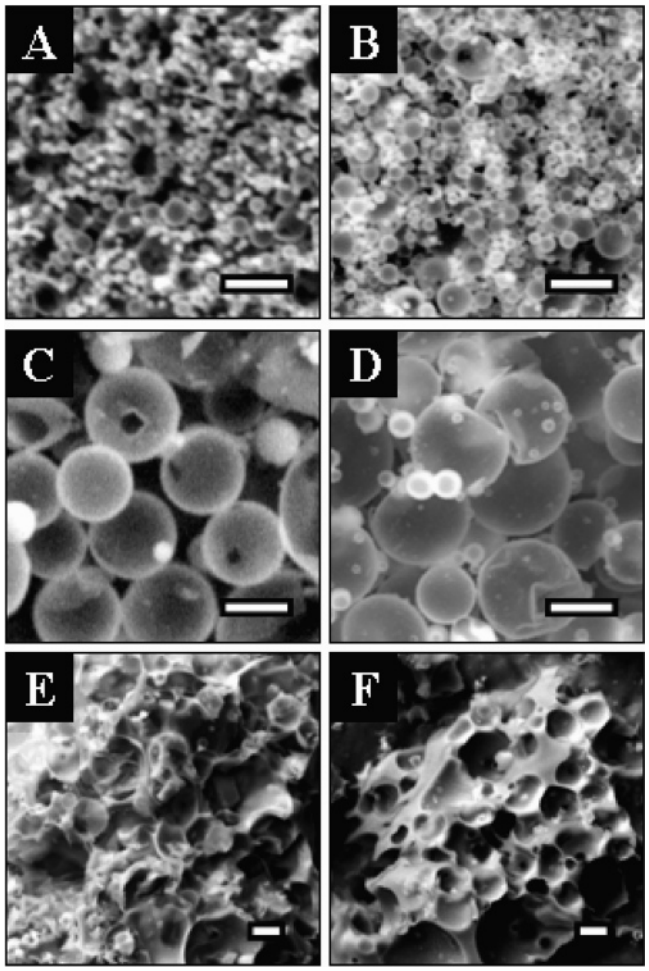

Figure 6. SEM images of L-SHHs at (A) 0.5, (B) 1, (C) 5, (D) 10, (E) 20, and (F) 40 mg mL^{-1} lysozyme concentration. Scale bars: (A−D) 5 μm, (E and F) 10 μm.

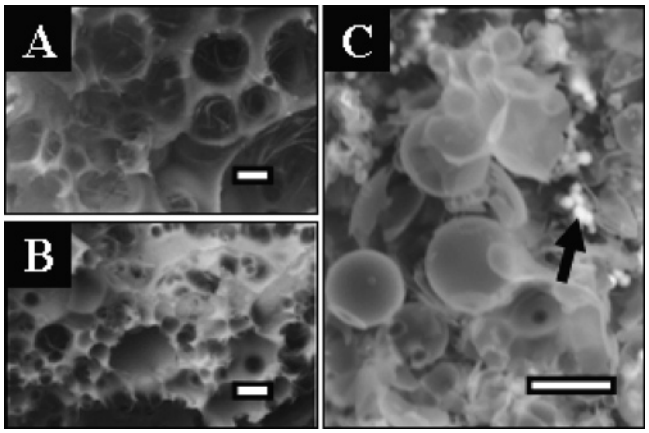

Figure 7. SEM images of the precipitates obtained at 2.0 mg mL^{-1} using (A) cytochrome C and (B) ribonuclease A, and SEM image at (C) 10 mg mL^{-1} of ribonuclease A. Scale bars: 10 μm.

concentrations, cytochrome C and ribonuclease A are not able to be adsorbed onto TEOS emulsion in enough quantity to assist inner-shell formation of the hollow shell structures, probably because of the weak foaming property. These proteins adsorbed loosely to the TEOS emulsion could act as glue between growing hollow structures. At high concentrations, ribonuclease A is likely to be localized around

(39) Arai, T.; Norde, W. *Colloids Surf.* **1990**, *51*, 1−15.

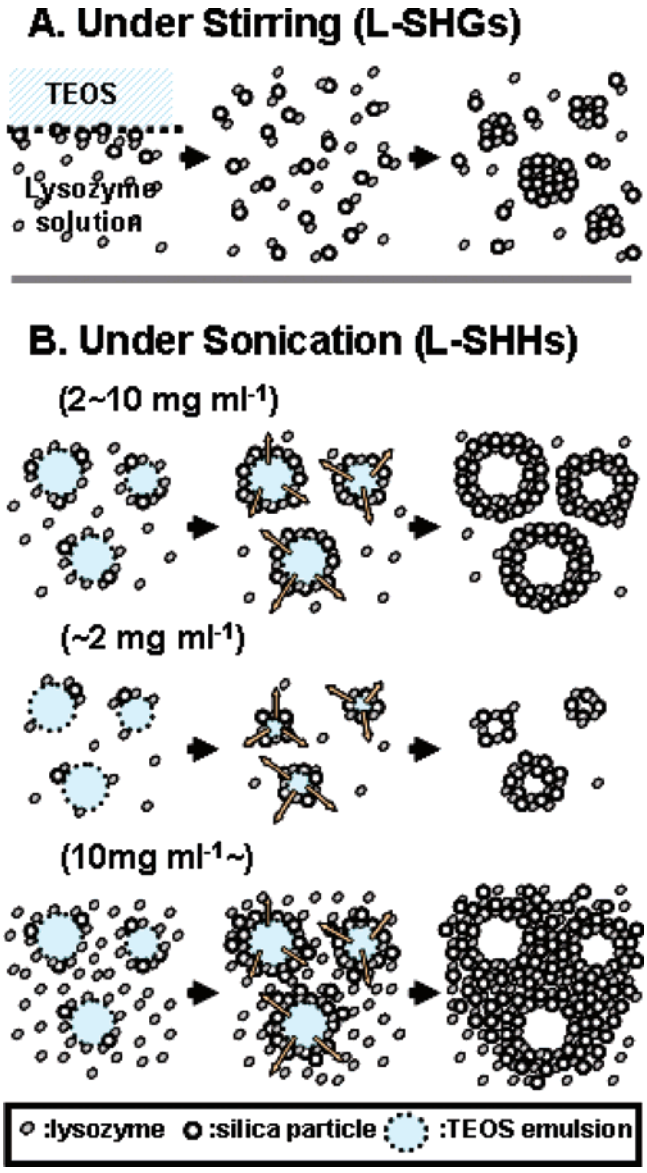

Figure 8. Proposed mechanism for the formation of (A) L-SHGs and (B) L-SHHs.

the TEOS emulsion, even though the interaction is not as strong as with lysozyme, leading to the formation of some granular particles. We conclude that a foaming property like that of lysozyme is essential to form a hollow structure using TEOS emulsion as a silica source.

Figure 8 is our proposed formation mechanism of L-SHGs and L-SHHs to explain how morphological controls were achieved by sonochemical treatment and an appropriate choice of lysozyme concentration.

With stirring, lysozyme molecules can come into contact with the TEOS only on the large-scale interface between the TEOS (oil phase) and the lysozyme solution (water phase) (Figure 8A). Subsequently, the primary lysozyme−silica particles are formed. Moderate stirring makes the primary silica−lysozyme particles break free into the water phase, after which continuous condensation occurs. When lysozyme is fully encapsulated within L-SHGs and does not remain in the reaction mixture at all, the growth of L-SHGs reaches a plateau at a particular particle size defined by the reaction condition. A granular shape quite similar to the L-SHGs reported here was produced by the action of lysozyme from TMOS as a silica source[14] and, interestingly, by a polyamine/phosphate mixture even from mono- and disilicic acid.[40] Therefore, the choice of silica sources and silica precipitating agents is perhaps not the most important factor contributing to different morphologies.

When sonication is used (Figure 8B), the interfacial area of the TEOS and lysozyme solution is expanded, as sonication induces dispersion of the TEOS emulsion. The foaming effect of lysozyme is thought to be a characteristic common to all ranges of lysozyme concentrations.[41] First, the TEOS emulsion generated by sonication is covered with lysozyme molecules (2 mg mL^{-1}~). When the lysozyme concentration is not sufficient to stabilize the TEOS emulsion (~2 mg mL^{-1}), the size of the emulsion droplets decreases with continuing sonication (Figure 6A and B). To confirm this effect of the sonication on producing a size decrease of L-SHHs, we carried out the L-SHHs formation experiment where the lysozyme solution was added to a presonicated mixture of TEOS and glycine buffer solution. SEM observation of the sample obtained demonstrated that hollow particles with a diameter of several tens of micrometers were formed. A similar size of TEOS emulsions was also observed after sonication by optical microscopy. These results proved that a decrease of the L-SHH's particle size occurred during sonication. Second, inner lysozyme−silica shell structures are formed on the surface of TEOS emulsion through the silica precipitation activity of lysozyme. These structures grow by trapping TEOS, which leaks thorough gaps in the lysozyme−silica shell on the outer surface. The presence of excess free lysozyme molecules causes the growing L-SHHs to combine with each other (10 mg mL^{-1}~), resulting in the formation of aggregation forms or spongelike structures (Figure 6E and F). Finally, when all lysozyme molecules are entrapped in shell structures, L-SHH formation is finished.

Conclusions

We have demonstrated that L-SHHs were successfully synthesized by the combination of a biomimetic approach and sonochemical treatment. The morphologies of particles can be controlled to be granular or hollow by altering the reaction conditions (stirring or sonication). The lysozyme−silica hybrid particles were formed only in weak basic solution. Probably, the balance of electrostatic and hydrophobic interaction between TEOS emulsion (silica) and lysozyme was optimized in this pH range. In particular, the morphologies of hollow structures were observed to be significantly influenced by the lysozyme concentration. Below a lysozyme concentration of 5 mg mL^{-1}, the particle diameter of L-SHHs increases with the increase in the lysozyme concentration. Above 10 mg mL^{-1}, aggregates form and a characteristic spongelike structure can be sometimes observed. Compared to other basic proteins, the

(40) Sumper, M.; Lorenz, S.; Brunner, E. *Angew. Chem., Int. Ed.* **2003**, *42*, 5192−5195.
(41) Beverung, C. J.; Radke, C. J.; Blanch, H. W. *Biophys. Chem.* **1999**, *81*, 59−80.

foaming property of the lysozyme molecule is thought to be necessary for the formation of hollow structures. The formation of L-SHHs is thus explained by the following steps: (1) A TEOS emulsion is generated by the sonochemical treatment and is stabilized by lysozyme. (2) Silica precipitation is induced by lysozyme only at the TEOS interface. (3) Lysozyme−silica hybrid shells are formed. The amount and the morphologies of precipitates are controlled by the lysozyme concentration in reaction solution.

The findings in this study support the view that silica precipitation activity and the morphological control effect are associated with each other but operate via different mechanisms. As a matter of fact, various morphologies of biosilica produced by the use of diluted silica precipitating agents have been reported.[42,43] However, it is well-known that a living cell generally contains macromolecules occupying 20−40% of the total volume.[44] Therefore, a crowded condition, that is, a reaction solution with a high concentration of silica precipitating protein, may well be a good mimic for the state of a silica mineralization process in vivo. Of course, although it should be stressed that in the work reported here sonochemical treatment is applied for morphological control, similar sorts of emulsion droplets assembled from organic molecules[45] could be an alternative to the TEOS emulsion in the above-mentioned model. We believe that our method using lysozyme as a typical example sheds new light on the creation of biopolymer-related materials with controlled morphologies.

CM071011V

(42) Patwardhan, S. V.; Mukherjee, N.; Steinitz-Kannan, M.; Clarson, S. J. *Chem. Commun.* **2003**, 1122−1123.
(43) Jan, J. S.; Lee, S.; Carr, C. S.; Shantz, D. F. *Chem. Mater.* **2005**, *17*, 4310−4317.
(44) Ellis, R. J. *Trends Biochem. Sci.* **2001**, *26*, 597−604.
(45) Sumper, M. *Science* **2002**, *295*, 2430−2433.